Abhijitkumar A. Jadhav
PhD Research Scholar
Visvesvaraya Technological University (VTU), Machhe, Jnana Sanagama
Belagavi, Karnataka, India, 590018
Dept. of Mechanical Engineering
India

Sanjay B. Zope
Professor
Sahyadri Valley College of Engineering & Technology, Rajuri, (Alephata)
Pune, Maharashtra, India, 412410
Dept. of Mechanical Engineering
India

Ravindra R Malagi
Professor
Visvesvaraya Technological University (VTU), Machhe, Jnana Sanagama
Belagavi, Karnataka, India, 590018
Dept. of Mechanical Engineering
India

Deepali A. Suryawanshi
Assistant Professor
Annasaheb Dange College of Engineering and Technology, Ashta
Sangli, Maharashtra, India, 416301
Dept. of Electrical Engineering
India

Design and Development of a Novel Tunable Electrorheological Fluid (ERF) Damper-foundation to Attenuate Residual Vibrations in Machine Tools

Residual vibrations in machine tools hamper accuracy and productivity. The attenuation of residual vibrations has been an industrial concern for decades. Meanwhile, the residual vibrations' vibration pattern reveals that the support foundation's damping capabilities predominantly influence them. Therefore, inserting dampers in any other location on a machine tool (such as a machine column) is ineffective. Hence, the scope of inserting the damper into the machine foundation needs to be verified. However, conventional machine mounting systems (concrete foundation and rubber mounts) equally respond to all variable inputs. Both these flocks resulted in inadequate dampening and perhaps poor accuracy. This paper provides a first-generation model of a semiactive-viscous damper (ERF damper-foundation) with tunable damping facilitating machine installation. Controlled experimentation by exposing the developed damper foundation to excitations of medium duty lathe machine confirms its effectiveness and obtains over 48% attenuation compared to a conventional concrete foundation.

Keywords: *Residual Vibrations, Tunable Damping, Electrorheological fluid (ERF), Viscous damper, Attenuation*

1. INTRODUCTION

Nowadays, the manufacturing industry expects faster, more stable, and more productive machine tools. This trend of adopting speedier machine tools demands using powerful drives to operate them. It resulted in a higher vibration level and a wider spectrum range compared to previous generations of machine tools. Typically, the cutting parameters, excitation-related to drive unbalances, and vibration attenuation techniques all impact the vibration response of any machine tool [1–3].

This paper presents a primary investigation for our mainstream research motivation. Machine tool vibrations are categorized as chatter and residual vibrations. During chip shearing, fluctuating cutting forces cause chatter vibrations, whereas machine tool movement, ground disturbances, and drive unbalance contribute to residual vibrations [1,2]. A common perception is that each of these vibrations has detrimental consequences [6]; chatter vibrations degrade the surface finish of the workpiece [3], whereas residual vibrations affect accuracy and productivity [4]. This perception is valid if the machine tool is installed on a passive concrete foundation; however, the outcome may be different if it is mounted on a foundation that may alter its dampening capacity. Previously, there had been very few attempts to install the machine tool on a tunable foundation, giving rise to this perception. So, the authors would like to develop a tunable damper foundation that installs machine tools and facilitates controlled damping, which may further be utilized to identify residual vibration's effect on the surface finish. Due to the detrimental effect of both vibrations, there is a persistent demand for innovative and efficient damping solutions for machine tools. As disclosed in earlier literature, a significant percentage of research has been devoted to offering a competitive solution to these problems [5–8].

Residual vibration is a rocking behavior (Fig.1) of the entire machine tool induced by its relative axial movement about the stable foundation on which it is installed [13]. It is essential to attenuate these low-frequency residual vibrations to enhance machining accuracy and productivity [9].

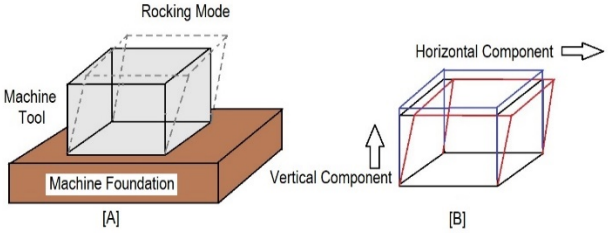

Figure 1. Illustration of a machine tool in rocking vibration mode.

While a comparative study on multi-point tool condition monitoring has been performed by Pradeepkumar et al. [45]. Meanwhile, Biju et al. [15] and Iwasaki et al. [16] proposed insertable dampers in machine columns to eliminate residual vibrations. On a similar note, Tomas et al. [17] inserted a flexible absorber claiming

Received: October 2022, Accepted: December 2022
Correspondence to: Abhijitkumar Anandrao Jadhav
Visvesvaraya Technological University (VTU),
Belagavi, India, 590018.
E-mail: abhijitkumarjadhav@gmail.com
doi: 10.5937/fme2301001J

30% suppression, and Rasid et al. [18] installed a tuned viscoelastic damper at the column of a milling machine that claimed 43% attenuation. However, the pattern of the residual vibrations reveals that they are significantly influenced by the damping capabilities of the machine foundation (support structure) rather than the damping opportunities at the machine columns [19,20]. As a result, the insertable dampers at the machine column are inefficient at dampening these low-frequency residual vibrations [21].

On the other hand, machine tools and their structures must be sufficiently stiff to withstand and prevent vib–rations induced by acceleration and unbalance at feed drives [22]. According to Khalaj et al. [23], rubber in–serts are one of the more successful ways to improve damping; nevertheless, they hamper the overall stiff–ness. As a result, there is an urgent need to improve dam–ping at the support foundation without sacrificing static stiffness to achieve substantial and effective dampening.

Two possible ways to do this are 1) Improving the structure and 2) Inserting dampers. Composite materials were introduced by Marichelvam et al. [24]. Akande et al. [25], steel and cast iron were used by Mohring et al. [26], entangled metallic wires were introduced by Zhu et al. [27], and Khalaj et al. [23] introduced a thin rubber sheet layer of soil for structural enhancement of a machine tool. Meanwhile, modifying the structure and foundation of existing machine tools is always tricky, making these techniques tough to adopt with existing machinery [28,29].

Researchers another option considered by resear–chers for improving support damping was the insertion of dampers. Both passive and active dampers can achieve this, and researchers employed both extensi–vely. Active dampers are usually more expensive and complicated than passive dampers [30]. Law et al. [5] used an electro-hydraulic actuator to implement active dampers, Kato et al. [31] used a pneumatic damper, and Preumont et al. [32] used a six-axis single-stage damper. Similar research on passive dampers that support mac–hine tools has been undertaken; for example, Geerts et al. [33] employed springs and rubber, Okwudire et al. [8] optimized isolator design, and Patel et al. [34] intro–duced multi-layer damping.

Despite extensive research to eliminate residual vib–ration [24,35,36], only a few studies have successfully regulated machine tool vibrations using a controlled damper [5]. This work proposes to design and fabricate a semiactive damper (SAD) whose dampening capa–bilities can be modified based on desired output while controlling input parameters and facilitating machine installation as a "mounting system." The proposed dam–per reacts in real-time to minute input signal changes while easily integrating with existing machines. It works on the principle of ER effect revealed by Whittle et al.[10], which is reversible and reveals a quick response time (a few milliseconds) con-cerning the applied electrical field, permitting tunable damping at SAD. The proposed SAD is called an "electrorheological fluid damper foundation" [ERFDF].

Conceptual designs are one of the most critical early stages of product development when solutions are generally established to meet the product's design requirements [37]. The authors intend to work on injecting viscous fluid into the foundation of a machine tool to improve damping while retaining stiffness (Not just retaining it, improved slightly).

Traditionally, there are two primary methods for installing a machine tool: 1) with a conventional static foundation (concrete foundation) and 2) with rubber mounts. Rubber mounts are now commercially available for quick installation of machine tools and mitigating residual vibrations, whereas concrete foundation has been well-known for decades. When paired with a machine tool, both techniques consistently respond to all variable inputs (like operating speed, workpiece and cutting tool materials, cutting parameters, machine type, cutting operation, and operators' skill). This constant response to all variable inputs resulted in suboptimal damping, and, as a result, the product manufactured with these machines could not attain optimum accuracy and surface finish [11, 46]. Considering this, there is an immediate need for a variable damper to serve as a machine mount to facilitate machine tool installation. As the authors wish to explore injecting fluid into machine foundations, adding ER fluid to the proposed damper foundation may also lead to variable and controllable damping. Overall, the proposed damper design is based on rubber mounts already commercially available on the market.

This research goes into the detailed design procedure of ERFDF, transforming the concept into a first-generation damper foundation model and arriving at various compositions capable of producing low-cost ER fluids. It validates the developed system's efficiency in reducing residual vibration when subjected to the excitation of a medium-duty lathe machine under controlled experiments and boundary conditions.

2. CHARACTERIZATION OF ERF

As mentioned in the previous section, variable damping at the proposed ERFDF was achieved by utilizing a unique feature of ERF, specifically its ability to modify its rheological properties in response to an electrical potential. Due to its unique features, the ERF has captivated the curiosity of researchers since its inven–tion by Winslow [39]. An ERF is a polarisable mixture of micro-sized, electrically nonconductive semicon–ductor particles or liquid crystal material with an elec–trically nonconductive carrier fluid. When no electrical potential is applied, the particle concentration in this composition must be low enough to keep the fluid viscosity relatively low. When an ER suspension is exposed to an external electric field of several kilovolts per millimeter, its rheological properties, such as viscosity, shear modulus, and yield stress, can change substantially.

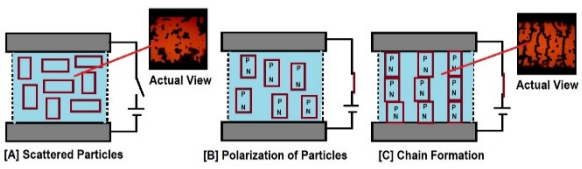

Figure 2. illustrates a depiction of the behaviors of ER particles before and after the application of an external electric potential

The ER phenomenon makes uniformly dispersed solid particles polarise when an electrical field is applied across such poles. Once polarised, they interact and form a chain-like structure parallel to the electrical field (Fig. 2) Hao et al. [40] hypothesized that a die–lectric loss model simplifies the ERF mechanism based on their experimental findings. This approach empha–sized two dynamic processes. The particle dielectric constant dominates the first stage of particle pola–rization. Along the second stage, known as particle turning, the polarised particle may be able to align in the path of the electric field. As the electrical potential increases, these chains begin to form a thicker column that inhibits fluid movement by becoming more viscous.

2.1 Ingredients to prepare low-cost ERF

Most ER fluids are non-polar and insulating liquids containing inorganic, non-metallic, organic, or poly–meric semiconductive components. There is various commercially available ERF; however, they are expen–sive. Due to the authors' emphasis on low-cost ERF, extensive research, analysis, and literature review cul–minated in a list of carrier fluids [Table 1] and particles [Table 2] used in different compositions to manufacture a range of low-cost ERF in the laboratory.

Table 1. Various carrier fluids are used for preparing numerous low-cost ERF in a laboratory

Sr	Carrier Fluids	Sr	Carrier Fluids
1	Alfa Silica	28	Alfa-Methacrylate
2	Alginic Acid	27	Mannitol
3	Alumina	28	Metallic Semiconductors
4	Aluminum Silica Mixture	29	Methoxyphenylimidoperylene
5	Aluminum Oleate	30	Methyl Acrylate
6	Aluminum Octoate	31	Methyl Methacrylate
7	Aluminum Stearate	32	Microcell-C
8	Arabic Gum	33	Microcrystalline Cellulose
9	Azaporhin Systems	34	Micronized Mica
10	Barium Titanate	35	Monosaccharides
11	Boron	36	Molecular Sieves
12	Cadmiumsulphidephosphor	37	N-Vinylpyrrolidole
13	Calcium Stearate	38	Nylon Powder
14	Carbon	39	Olefins
15	Cellulose	40	Onyx Quartz
16	Ceramics	41	Phenol formaldehyde Polymer
17	Charcoal	42	Phthalocyanine
18	Chloride	43	Polystyrene Polymers
19	Colloidal Kaolin Clay	44	Porhin
20	Crystalline Silica	45	Phosphototungstomolybic Acid
21	Crystalline D-Sorbitol	46	Polymethacrylate Mixture
22	Di-allyl ether	47	Polyvinyl Alcohols
23	Dimethyl Hydantoin Resin	48	Pyrogenic Silica
24	Diethylcarbocyanineodide	49	Quartz
25	Divinylbenzene	50	Rottenstone
26	Dipheylthiazoleanthraquinone	51	Rubber
27	Dyes	52	Silica Gel Powder

Table 2. Various particles are used for preparing numerous low-cost ERF in a laboratory

Sr	Particles	Sr	Particles
1	Aldehydes	20	Grease
2	Aliphatic Esters	21	Ketones
3	Aroclor	22	Kerosene
4	Carbon Tetrachloride	23	Linseed Oil
5	Castor Oil	24	Liquid Paraffin
6	Diphenyl Sulphoxides	25	Mineral Oil
7	Chloroform	26	Nitrobenzene
8	Cotton Seed Oil	27	Olefins
9	Di-Ethylhexyl Adipate	28	Olive Oil
10	Dielectric Oil	29	Orthochlorotoluene
11	Different types of Ethers	30	Polyalkylene Glycols
12	Diphenyl Ethers	31	Polychlorotrifluoroethylene
13	Diphenyl Sulphones	32	Polychlorinated Biphenyls
14	Dibutyl Sebacate	33	Resin Oil
15	Fluorinated Hydrocarbons	34	Silicone Oils
16	Fluorinated Polymers	35	Transformer Oil
17	Fluorolube	36	Trifluorovinyl Chloride
18	Fluoro-silicones	37	White Oils
19	Chlorobentzenediphenyl Alkenes	39	Xylene

2.2 Ingredients to prepare low-cost ERF

To explore and analyzing the efficacy of ERFDF, three samples of ERF fluid are prepared to utilize a combi–nation of three different particles and silicon oil as the carrier fluid. The best of these three samples is picked based on the viscosity test, sedimentation test, and voltage breakdown analysis results. Table 3 summarises the content and outcomes of the trials mentioned above.

Based on its superiority among the three combi–nations, a carrier liquid, "silicon oil," with a 22% by-weight percentage of "Arabic gum" particles, was selected for use in the proposed ERFDF.

3. DESIGN AND DEVELOPMENT OF ERFMM

3.1 Design strategy

The ERFDF design and development process is cha–llenging due to the numerous physical and geometrical constraints. Among the numerous constraints identified are the following: a massive static and dynamic load of the machine tool, three directional displacements of vibration amplitude, constrained motions, the height of ERFDF (since ERFDF is placed below the machine tool), compactness required, adaptability required, application of high voltage DC supply, electrical insulation requirement. The multiple iterations resulted in the development of ERFDF's first-generation prototype. Figure 3 depicts the concept's evolution into the first-generation prototype of ERFDF.

The ERFDF has a piston-cylinder configuration. The ERFDF's exterior cup (outer cylinder) is a fixed elec–trode. At the same time, the piston is a moving electrode that serves as a machine tool mounting arrangement. The ERF is injected into the cavity gap between these two electrodes to facilitate the initiation of solid-to-liquid transition upon application of an electrical potential. The electric interface channel –connects positive and negative electrode terminals to external power sources.

Table 3. Different compositions of ERF samples selected for testing and implementation in ERFDF

Carrier Fluid	Carrier Fluid Quantity (ml.)	Particles	Particles Quantity (gm)	Density [g/cm2]	Kinematic Viscosity [centistokes]	Dynamic Viscosity [centipoises]	Dielectric strength in AC [kV/ mm]	Strength in DC [kV/mm]	Sedimentation Time
Silicon Oil	930	Silica Gel	70	0.2944	35.87	66.36	2	2.5	Low
	920	SiO2	80	0.2837	26.35	49.13	7.2	9	Moderate
	800	Arabic Gum	176	0.3024	28.08	53.352	7.6	9.5	Highest

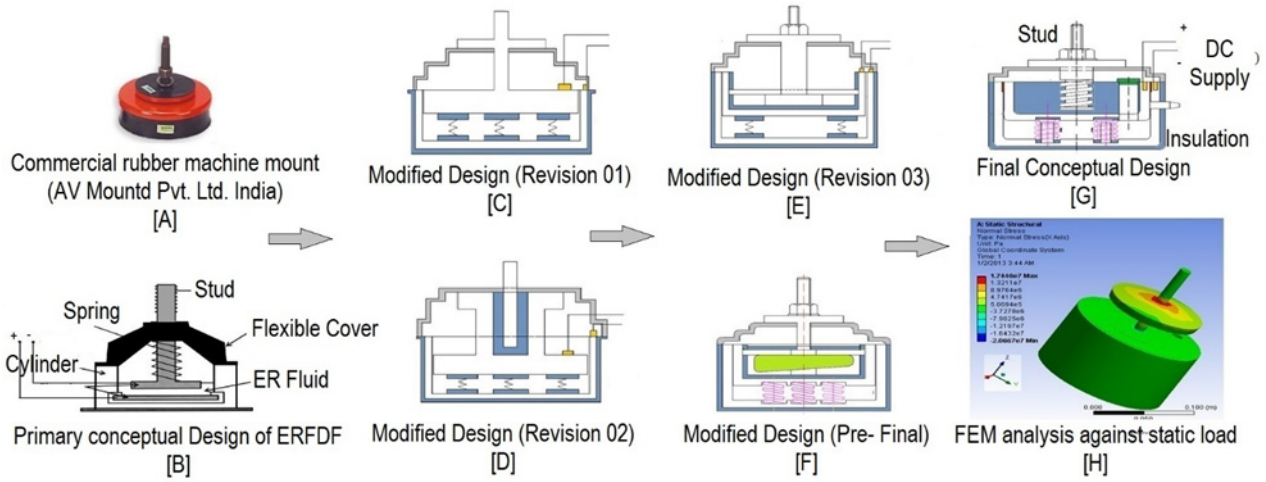

Figure 3. Conceptual design, development, and modifications of ERFMM and its stepwise progress

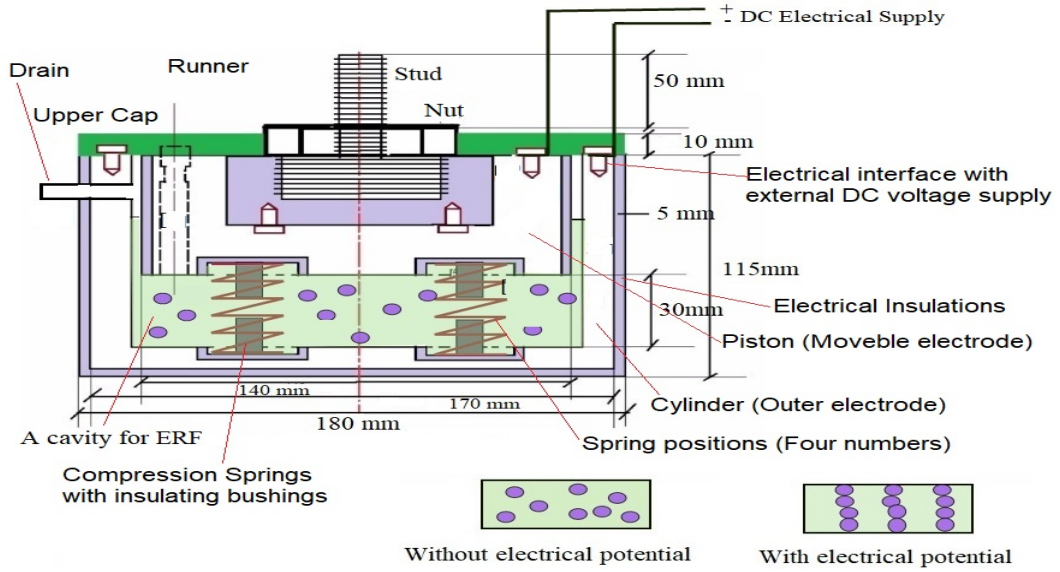

Figure 3. The ERFMM's layout with different components

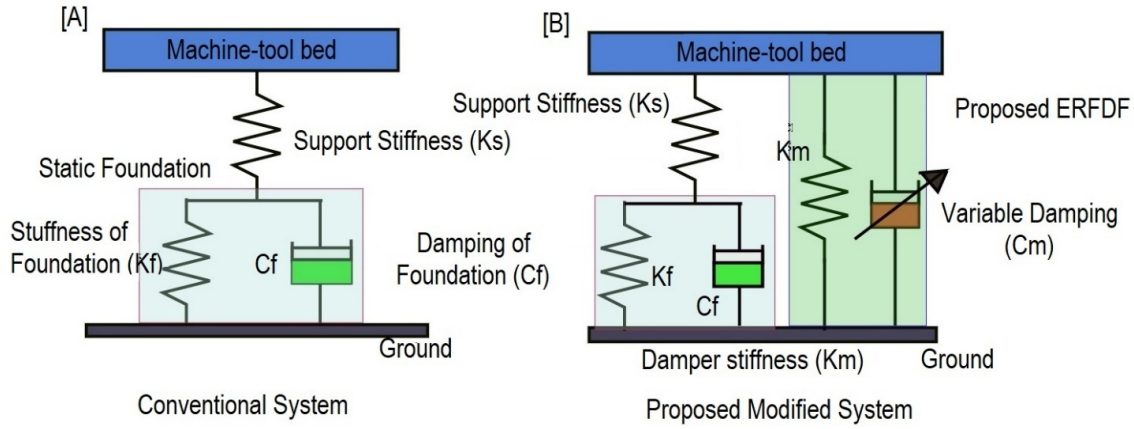

Figure 5 The modeling of machine tool and ERFMM; a) Conventional machine foundation system b) Proposed viscous ERFMM and machine tool system.

A 2.5 mm gap around the circumference between the piston electrical electrode and the outer cup electrode maintained sufficient electrically induced strength (high voltage DC). The outer cup, piston, stud, and support plate are made of plain carbon steel (40C8), while the compressive springs are constructed of medium-carbon steel. Furthermore, because ERF is exposed to a high-voltage DC supply (0 kV to 8 kV), proper electrical insulation is guaranteed during the design process. ERFDF maintains a layer of polytetrafluoroethylene (PTFE) in crucial areas because it is an effective electrical insulator due to its high dielectric strength and low dissipation factor. The appropriate failure theories are applied to the technical design of the individual components, which are then validated using FEA for static loading conditions [41,42]. Figure 4 depicts the ERFDF's final design and significant dimensions.

Compressive spring deflection is limited to the y-axis, whereas guide bushings within the ERFDF limit movement in the x- and z-axis direction. In addition, Table 4 offers a few essential design parameters and nomenclatures for the ERFDF.

The stiffness of the external damper is typically less than that of the machine tool table support and foun-dation. According to the traditional design, the machine support, foundation, and supplementary external support /damper for enhancing damping (if available) are all connected in series. As a result, the overall stiffness of the support is lowered. To dampen overall residual vib–rations, both support stiffness and support damping must be optimized. The ERFDF is connected to the proposed system's con–ventional foundation to preserve total support stiffness and produce superior damping. Figure 5 depicts the con–ventional and proposed machine tool system with ERFDF.

Table 4. Essential design parameters of ERFMM

Parameters and nomenclature	Quantity
Mass of lathe machine tool under experimentation(M)	700 kg
Weight of lathe machine under experimentation	6867 N
Spring wire diameter	0.00316 m
Mean diameter of the stud	0.012 m
The diameter of an enlarged portion of the stud	0.024 m
Maximum height of mount	0.130 m
Static force due to weight on a single MTM (Fstatic)	429.06 N
Static deflection (δ)	3.16 x 10-3 m
Spring constant for four springs at single MTM (k)	5.43 x 105 N/m
Equivalent spring constant (K	2.17 x 106 N/m
Damping constant of single MTM (c)	480.685 N-s/m
Equivalent damping coefficient (C)	1922.74 N-s/m
Theoretical Natural Frequency (ω_n)	8.86 Hz
Critical damping coefficient (Cc)	77992.79 Ns/m
Damping coefficient/ Damping factor (ζ)	0.0246
Dielectric strength in AC supply	19 kV
The gap between the two electrodes	0.0025 m
Dielectric strength with AC supply	7.6 kV/ mm
Dielectric Strength with DC supply	9.5 kV/mm

3.2 Governing equation of motion

Eq.1 depicts the general equation of motion for a mec–hanical system that includes a machine tool and the proposed ERFDF under investigation. The y-direction displacement of the machine tool is of considerable magnitude. In contrast, motion is constrained in the x and z- directions. Therefore, the displacement magni–tudes in the x-direction and z-direction are excluded from this analysis.

$$m\ddot{u}_y + C_e\dot{u}_y + k_e u_y = P \tag{1}$$

Eq. 1 is further modified as follows,

$$m\ddot{u}_y + \left(C_f + C_m\right)\dot{u} + \left(k_f + k_m\right)u = \Delta_1 P + \Delta_2 P + \Delta_3 P + \Delta_4 P \tag{2}$$

where, $\Delta_1 P$: The force of friction, $\Delta_2 P$: The force ge–nerated due to the cutting process, $\Delta_3 P$: The force gene–rated due to change in the shear phase, $\Delta_4 P$: The variable unbalanced force is influenced by a drive source, Cf: equivalent damping coefficient of foun–dation, Cm: damping coefficient of ERFDF, kf: Stiffness of foundation, and kf: Stiffness of ERFDF.

At the initial stages of experimentations, only the excitation associated with the unbalance force instigated due to a drive disruption is considered for the study and proposed to attenuate the vibrations associated with the drive's excitement. The other type of excitation is con–sidered at the next stage of experimentation, which is separate from this paper; hence these excitations are neglected.

$$\Delta_1 P = 0, \Delta_2 P = 0, \Delta_3 P = 0 \tag{3}$$

The damping force of the proposed system varies due to the use of controllable rheological properties of ERF when exposed to electrical protentional. Hence, equation (04) introduces a term for the ER effect coefficient.

$$m\ddot{u} + \left(C_f + E_t C_m\right)\dot{u} + \left(k_f + k_m\right)u = \Delta_4 P \tag{04}$$

where E_t is the ER effect coefficient, its value is further calculated in line with the experimental investigation mentioned by Kim et al. [41]. As ERF is field sensitive to the electric field; hence the yield stress and viscosity dramatically vary in the presence of electrical potential. The shear stress in ERF is the composition of the field-independent shear stress (ζNE)and the field-dependent part (ζE), based on the Bingham model [42]

$$\zeta\left(E\right) = \zeta_{NE} + \zeta_E \tag{5}$$

where $\zeta_{NE} = \eta$ and $\zeta_E = \alpha E^{\beta}$ The α and β are constants that depend on the inherent properties of ERF and are determined experimentally. Kim et al. have experi-mentally investigated the values of the α and β for a particular composition of the ERF. Similarly, the values are α = 427, β =1.2, and η = 30 cSt at room temperature experimentally investigated for the composition selected for ERFDF. These values are further used to determine the ER effect coefficient (E_t), which is used for further calculations in the dimensional analysis (DA) module. The DA is not a part of this manuscript.

4. EXPERIMENTATIONS

4.1 Experimental setup

Simulating the complex excitation pattern of a specific machine tool using an artificial vibration exciter is difficult. The magnitude necessary to excite a developed ERFDF is on the higher side, necessitating an exciter of higher quality. Due to the unavailability of such a specific exciter forced to use a medium-duty lathe as an exciter. The proposed experimental setup consists of a medium-duty lathe (Make: Anapurna) machine with all attachments and accessories mounted using an ERFDF at one of the four corners and a conventional static foundation at the remaining three corners. Figure 6 shows the proposed experimental setup.

The excitation associated with an unbalanced drive force is only examined at the beginning of the research, followed by the excitation connected with the turning operation, which is outside the scope of this article. The actual experimentation for this study is conducted in two phases. Initially, a lathe machine is installed on a conventional four-cornered static foundation. This experimental model is referred to as a "Static Condition" in both the experiment and the analysis. N=222.06 rpm, 363.36 rpm, 547.36 rpm, and 842.36 rpm are permissible idle speeds for a lathe machine.

During the second phase of the experiment, a single ERFDF is installed in one of the four corners to determine the effectiveness trend of ERFDF and the magnitude of vibration attenuation using a single ERF viscous damper foundation. This strategy is referred to as a quarter-machine model.

In subsequent rounds of investigation, the number of dampers would be raised from one to four. It leads to experiments using schematic models as half, three-quarters, or full models. Figure 7 represents the various schematic models using machine footprints. During the quarter model condition, proper care has ensured for installing machine-tool using water level indicators.

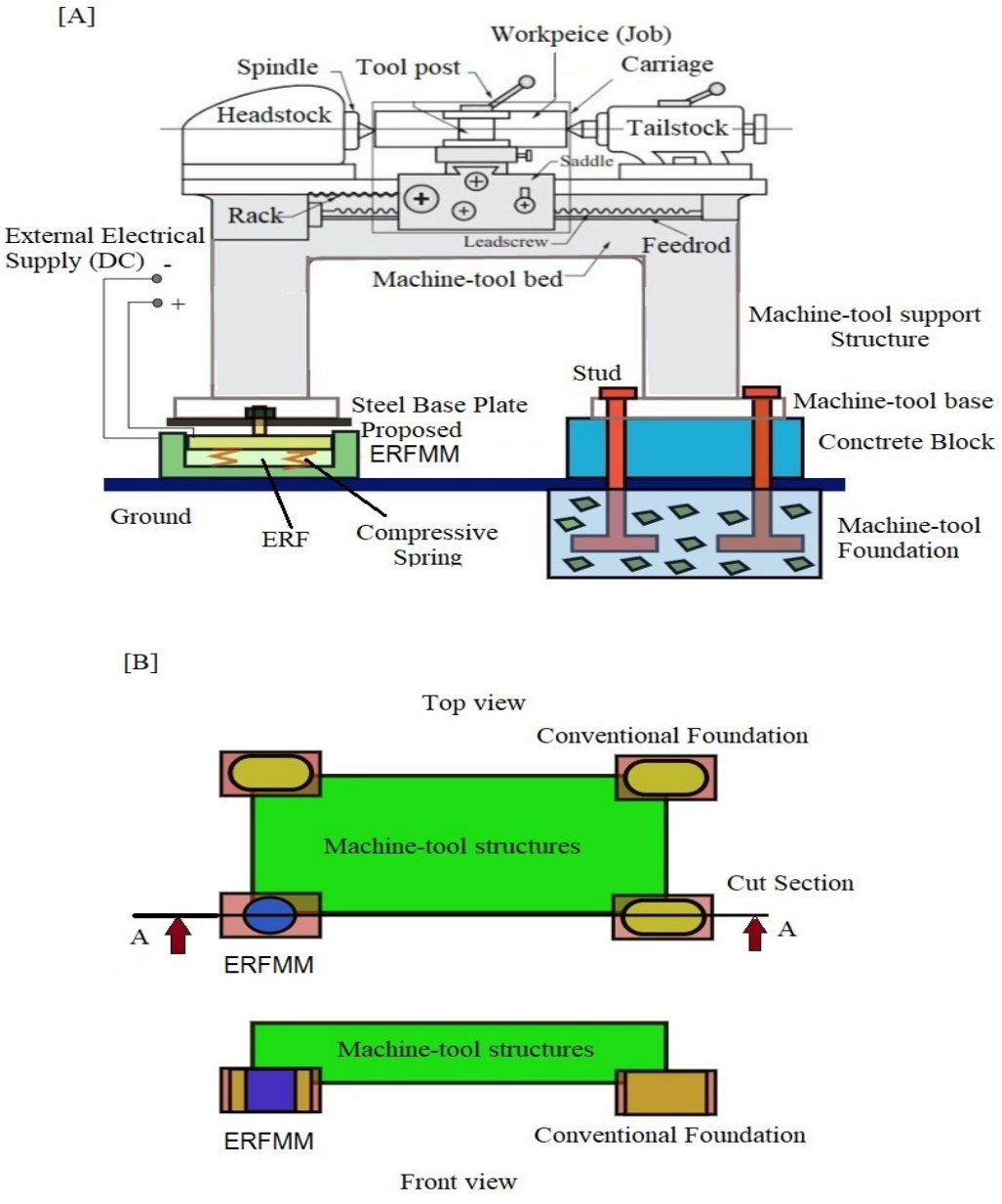

Figure 4 [A] Schematics of lathe machine used in experimentation with ERFMM [B] Schematic front and top view of an experimental setup

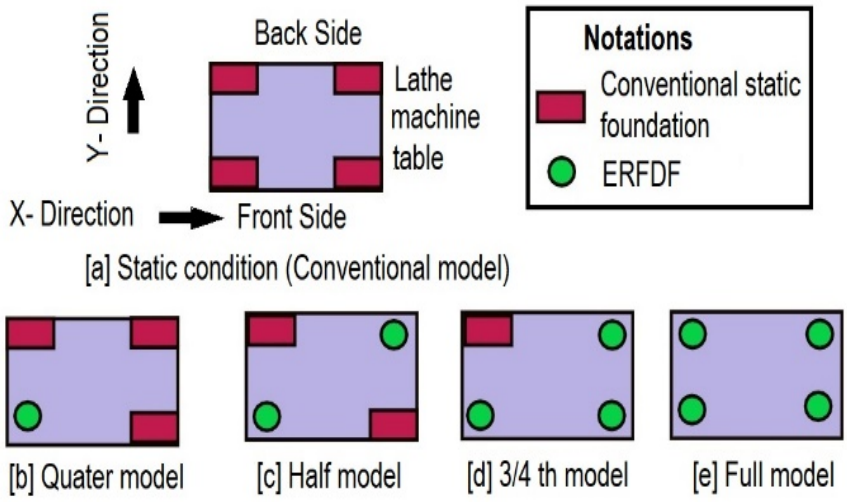

Figure 7 Footprints of lathe machine used in study a) Static condition (Conventional model) b) Quarter model c) Half model d) ¾ model and e) Full model

Figure 8 Experimental setup to obtain the response of the ERFMM used to mount a lathe machine (quarter machine model)

It also ensures equal load distribution to support all four corners of a lathe machine. The required quantity of ERF is injected inside the cavity of the EFFDF. Electrical potential difference is applied across the pole of the ERFDF through an electrical interface and external high-voltage supply source. The lathe machine makes an idle run at various speeds N=222.06 rpm, 363.36 rpm, 547.36 rpm, and 842.36 rpm. The Potential difference across the pole is also varied from voltage V = 0kV, 2kV, 4kV, 6kV, and 8kV. The vibration signals of the lathe machine are collected through the acceleration transducer, which is pre-fixed on one of the support legs of the machine table in the y-direction. The data collecting instrument from Brüel&Kjær Sound & Vibration company (sampling frequency is 120 HZ) is used. During an idle run, real-time machine-tool vibration was captured with and without a damper, with ERF effect and without ERF effect. FFT analyzer, along with an accelerometer, is used for capturing dynamic parameters in the form of the frequency domain. The experimental set up shown in Figure 8.

5. RESULTS AND DISCUSSION

5.1 The comparison between the theoretical and experimental natural frequencies of the system

The theoretical natural frequency is computed with known mass quantities and equivalent spring stiffness. At the same time, the experimental values natural frequency of the system under consideration is obtained after the impact test. Figure 9 illustrates the collected spectrum of natural frequency. The system's theoretical and experimental natural frequencies are 8.86 Hz and 7.76 Hz, nearly equivalent at specified boundary conditions.

5.2 The suppression effects of ERFMM at various speeds and applied potential

The vibration response of a machine tool and quarter model of ERFDF is captured in the auto spectrum [Frequency (Hz) vs. amplitude (mm/s2)] by an FFT analyzer to evaluate the effectiveness of the design of an ERFDF in attenuating machine-tool vibrations. Each configuration, mounting condition, operating speed, and applied electrical potential have a unique vibration response. As a result, each condition receives its auto spectrum. As a result, 24 auto spectrums in the frequency range of 0 to 100 Hz and 5616 amplitudes were acquired for analysis. These auto spectra were recorded for two mounting machine conditions, static and quarter machine models, with speed variations of 222, 363, 547, and 842 rpm with applied electrical potentials of 0kV, 2kV, 4kV, 6kV, and 8kV. It's tough to illustrate all 24 spectrums here; only two sample auto spectrums are shown. Figure 10 depicts the auto spectrum captured at quarter machine condition, 222 rpm speed, and 2 kV applied electrical potential in a frequency range of 0 Hz to 100 Hz. This auto spectrum indicates the response amplitude of 30.29, 34.68, 34.91, and 48.65 in mm/s^2 at 8.73 Hz, 41.31 Hz, 70.25 Hz, and 82.62 Hz, respectively.

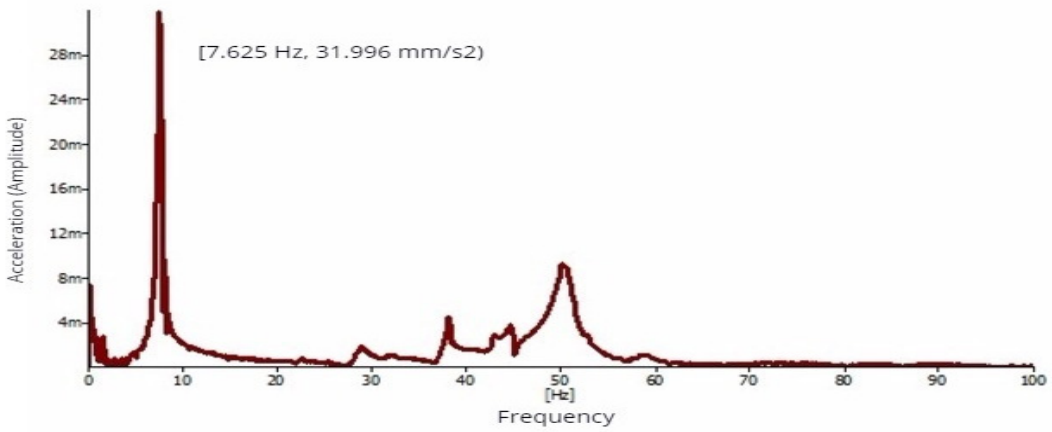

Figure 5 The auto spectrum captured during the impact hammer test to determine the natural frequency of the lathe machine and ERFMM system

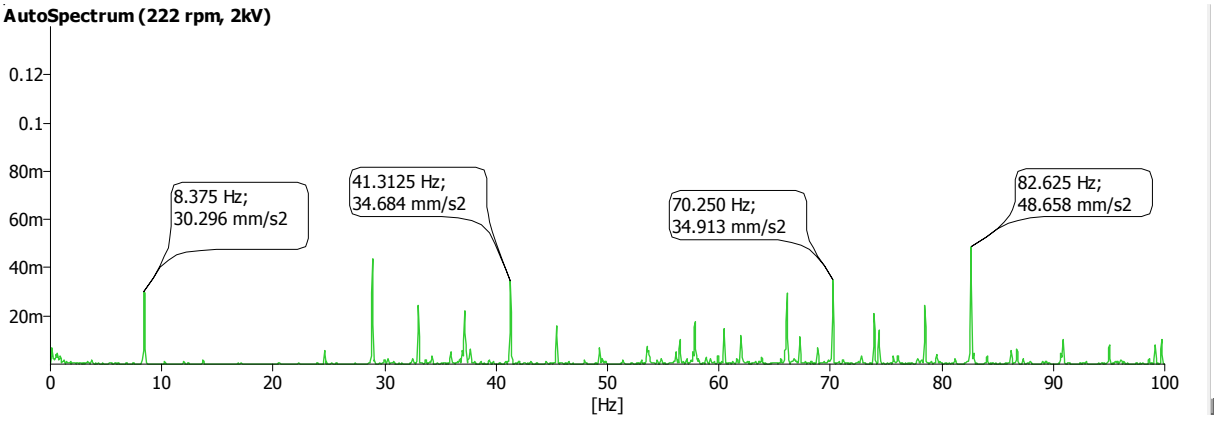

Figure 60 Autospectrum of frequency vs. vibration amplitude (mm/s2) at a speed of 222 rpm and 2 kV applied potential

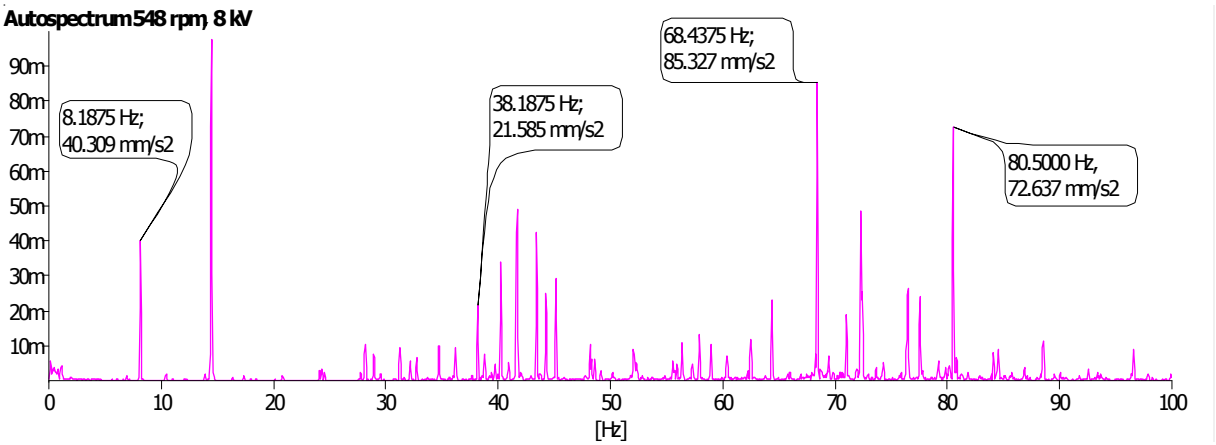

Figure 7 Auto spectrum of frequency vs. vibration amplitude (m/s2) at a speed of 548 rpm and 8 kV applied potential

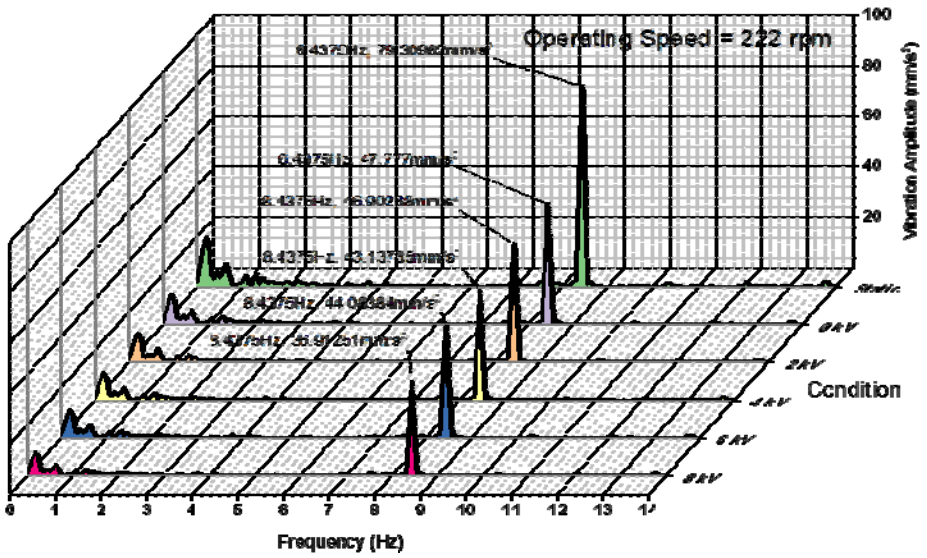

Figure 8 Comparative plot exhibiting the effectiveness of developed ERFMM at a speed of 222 rpm

On a similar line, one more auto spectrum for the one ERFDF at one corner of the lathe machine at 548 at 8 kV applied potential across the electrical pole is illustrated in fig. 11. This auto spectrum indicates 40.30, 21.58, 85.32, and 72.63 mm/s^2 vibration amplitude at 8.18, 38.18, 68.43, and 80.5 Hz, respectively. Table 5 represents the relative vibration amplitude at numerous conditions with excitation frequency, speed, and applied electrical potential.

The reduction in vibration amplitude is proven for a given dominating excitation frequency. These spectra were examined in various ways, initially comparing vibration amplitude (mm/s^2) at a few dominating frequencies. These results are favorable when compared, as utilizing ERFDF in certain conditions resulted in focused abatement of residual vibrations. For example, figure 12 depicts a comparative overlapping spectrum from 0 to 14 Hz at an operating speed of 222 rpm under various conditions (Static, 0 kV, 2 kV, 4 kV, 6 kV, and 8 kV).

Suppose a dominant natural frequency (8.4375 Hz) is selected for comparison in this boundary condition. It demonstrates the effectiveness of the ERFDF in attenuating residual vibrations. The vibration amplitude reduced significantly from 79.30 mm/s^2 to 36.91 mm/s^2 stepwise compared to static condition to 8 kV applied electrical potential across the pole of ERFDF. Nume–rous such comparative studies have been undertaken, and numerous plots have been drawn (Not included in the manuscript) to confirm the efficacy of ERFDF.

Table 5. Vibration amplitude at various conditions

Frequency [Hz]	Speed [rpm]	Vibration Amplitude (mm/s^2)					
		Static Condition	0 kV	2 kV	4 kV	6 kV	8 kV
3.75	222	1.91	1.13	1.13	1.09	1.06	0.89
6.12	363	32.36	19.50	19.14	17.60	17.20	15.06
9.18	547	103.60	62.41	61.28	56.36	55.48	48.22
14.56	842	155.62	93.60	92.19	84.79	82.56	72.55

Another method of evaluating the efficacy of ERFDF is to compare the highest amplitude (mm/s^2) recorded at the specific condition in a given frequency band (0 to 100 Hz).

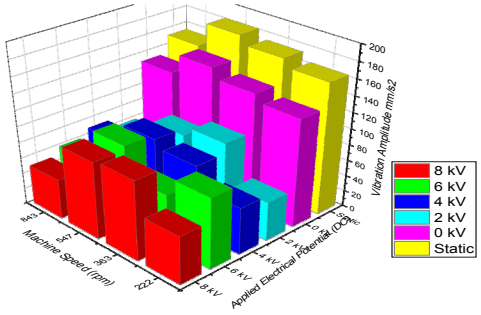

Figure 13 The effectiveness of ERFMM considering the highest peak at a given particular condition

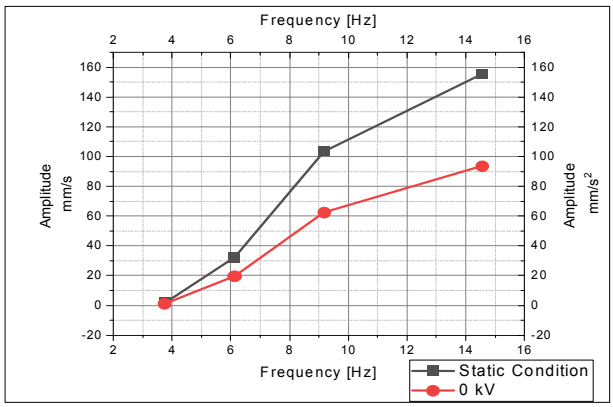

Figure 14 The effectiveness of ERFDF comparing static condition and 0 kV applied potential.

Figure 13 compares maximum amplitudes measured under various situations, regardless of the excitation frequency. At all speeds tested, a machine tool and ERFDF response produced an amplitude decrease of 33.76% compared to a conventional foundation at a 0 kV potential difference [fig. 14], on a similar line with a 45.66% amplitude reduction at 2kV [fig. 15], a 45.90% amplitude reduction at 4kV [fig. 16], a 46.37% amplitude reduction at 6kV [fig. 17], and a 48.37% amplitude reduction at 8kV [fig.18].

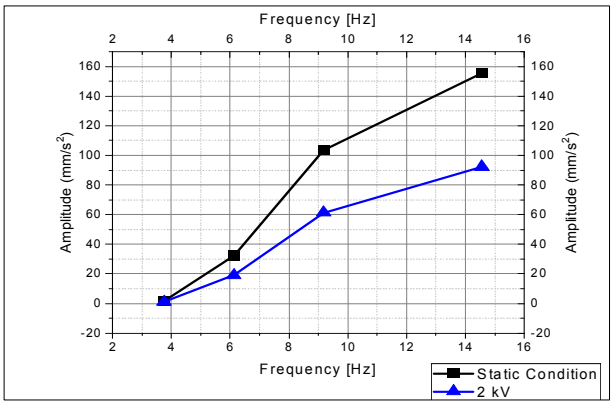

Figure 15 The effectiveness of ERFDF comparing static condition and 2 kV applied potential.

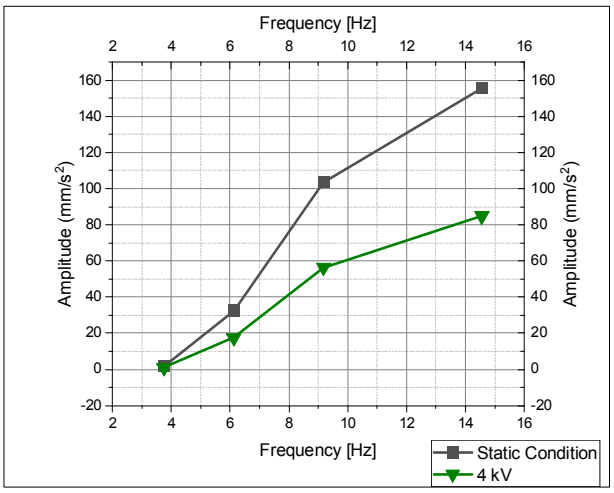

Figure 16 The effectiveness of ERFDF comparing static condition and 4 kV applied potential.

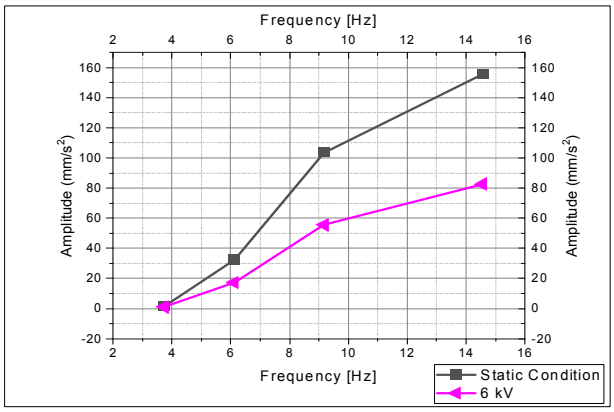

Figure 17 The effectiveness of ERFDF comparing static condition and 6 kV applied potential.

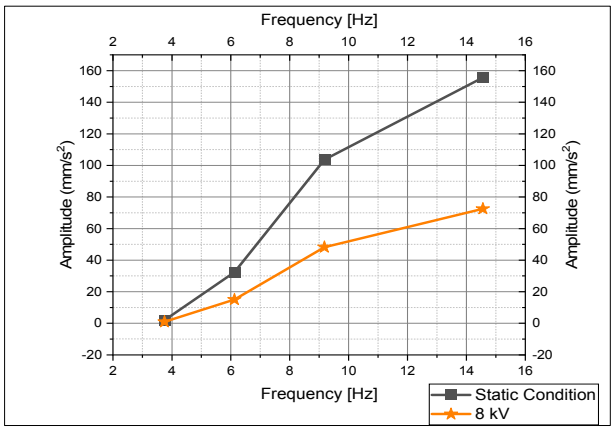

Figure 18 The effectiveness of ERFDF comparing static condition and 8 kV applied potential.

6. CONCLUSION

ERFDF's first-generation model has been successfully designed and built. A numerical model of a machine tool mounted with a quarter machine model and one ERFDF was developed using the DA and solved in Microsoft Excel to obtain theoretical results. To validate an ERFDF first-generation model, an experimental study is carried out on it, exposing it to the excitation of a lathe machine. The current work offers a semiactive damper with tunable damping and is convenient for machine tool mounting to mitigate residual vibrations.

The developed ERFDF can also attenuate residual vibrations. The experimental data generated is trained and tested for various application scenarios. The obtained results are summarised below.

- The residual vibration hampers the accuracy and productivity of a machine tool. The attenuation of these residual vibrations is possible through the optimum value of stiffness and damping at the machine foundation than at any other location on a machine tool.
- The proposed tunable semiactive damper (ERFDF) facilitating machine mount is successfully designed and developed.
- The developed ERFDF was successfully used in attenuating residual vibrations. Compared with the static condition, the developed system provides 48 % more attenuation in a quarter machine model condition.
- As the running speed of a lathe machine increases, the vibration amplitude increases linearly, affec–ting the system dynamics. While the vibration am–plitude reduces significantly with increasing applied potential difference from 0 kV to 6 kV. While the amplitude reduces slightly if applied electrical potential changes from 6 kV to 8 kV.

The trials were conducted with an ERFDF while exposing it to the excitation of a lathe machine during an idle running condition and while performing a turning operation at different conditions. As mentioned earlier, 24 auto spectrums mentioning a frequency vs. amplitude graph were captured in idle conditions at 5616 excitation frequencies, and 96 auto spectra were during a turning operation. In the future scope of research, the experimental data is further used to develop an experimental-data-based model (EDBM). The EDBM further develops with Dimensional analysis (DA) using Buckingham Pi Theorem (BPT) to arrive at a mathematical equation for predicting vibration amplitude and surface finish.

ACKNOWLEDGMENT

The authors like to acknowledge the support extended by Prof. R.A. Kanai [Executive Director, ADCET, Ashta], Dr S.S. Gawade [RIT, Sakharale], Dr S.B.

Kumbhar [RIT Sakharale], Dr R.G. Desavale [RIT, Sakharale], Dr Prasad Shinde, Dr V.B. Patil, Prof. M.M. Jadhav, Prof. A.M. Pirjade, Faculties of ADCET and central workshop staff [ADCET, Ashta].

REFERENCES

[1] U. Heisel, M. Gringel, Machine Tool Design Requirements for High-Speed Machining, CIRP Ann. 45 (1996) 389–392. https://doi.org/10.1016/S0007-8506(07)63087-X.

[2] N. Ahobal, S.L. Ajit prasad, Study of vibration characteristics of unbalanced overhanging rotor, IOP Conf. Ser. Mater. Sci. Eng. 577 (2019) 012140. https://doi.org/10.1088/1757-899X/577/1/012140.

[3] S. Qin, L. Zhu, M. Wiercigroch, T. Ren, Y. Hao, J. Ning, J. Zhao, Material removal and surface gene–ration in longitudinal-torsional ultrasonic assisted milling, Int. J. Mech. Sci. 227 (2022) 107375. doi.10.1016/j.ijmecsci.2022.107375.

[4] R. Kishore, S.K. Choudhury, K. Orra, On-line control of machine tool vibration in turning opera–tion using electro-magneto rheological damper, J. Manuf. Process. 31 (2018) 187–198. https://doi.org/10.1016/j.jmapro.2017.11.015.

[5] M. Law, M. Wabner, A. Colditz, M. Kolouch, S. Noack, S. Ihlenfeldt, Active vibration isolation of machine tools using an electro-hydraulic actuator, CIRP J. Manuf. Sci. Technol. 10 (2015) 36–48. https://doi.org/10.1016/j.cirpj.2015.05.005.

[6] H. Wu, Y. Wang, M. Li, M. Al-Saedi, H. Handroos, Chatter suppression methods of a robot machine for ITER vacuum vessel assembly and maintenance, Fusion Eng. Des. 89 (2014) 2357–2362. https://doi.org/10.1016/j.fusengdes.2014.02.007.

[7] C. YUE, H. GAO, X. LIU, S.Y. LIANG, L. WANG, A review of chatter vibration research in milling, Chinese J. Aeronaut. 32 (2019) 215–242. https://doi.org/10.1016/j.cja.2018.11.007.

[8] J. Lee, C.E. Okwudire, Reduction of vibrations of passively-isolated ultra-precision manufacturing machines using mode coupling, Precis. Eng. 43 (2016) pp. 164–177. https://doi.org/10.1016/j.precisioneng.2015.07.006.

[9] G. Bianchi, S. Cagna, N. Cau, F. Paolucci, Analysis of Vibration Damping in Machine Tools, Procedia CIRP. 21 (2014) 367–372. https://doi.org/10.1016/j.procir.2014.03.158.

[10] A. Ast, S. Braun, P. Eberhard, U. Heisel, Adap–tronic Vibration Damping for Machine Tools, CIRP Ann. 56 (2007) 379–382. https://doi.org/10.1016/j.cirp.2007.05.088.

[11] D. Li, H. Cao, X. Chen, Active control of milling chatter considering the coupling effect of spindle-tool and workpiece systems, Mech. Syst. Signal Process. 169 (2022) 108769. https://doi.org/10.1016/j.ymssp.2021.108769.

[12] M. Ozsoy, N.D. Sims, E. Ozturk, Robotically assisted active vibration control in milling: A feasibility study, Mech. Syst. Signal Process. 177 (2022) 109152. https://doi.org/10.1016/j.ymssp.2022.109152.

[13] V.I. Kochergin, S.P. Glushkov, Improvement of Machine Protection against Vibration, Transp. Res. Procedia. 61 (2022) 674–680. https://doi.org/10.1016/j.trpro.2022.01.107.

[14] P. Boscariol, D. Richiedei, I. Tamellin, Residual vibration suppression in uncertain systems: A robust structural modification approach to trajec–tory planning, Robot. Comput. Integr. Manuf. 74 (2022) 102282. https://doi.org/10.1016/ j.rcim.2021.102282.

[15] C.V. Biju, M.S. Shunmugam, Performance of magnetorheological fluid based tunable frequency boring bar in chatter control, Measurement. 140 (2019) 407–415. https://doi.org/10.1016/j. measu–rement.2019.03.073.

[16] M. Iwasaki, N. Hirose, M. Kawafuku, H. Hirai, Residual vibration suppression using initial value compensation for repetitive positioning, in: 8th IEEE Int. Work. Adv. Motion Control. 2004. AMC '04., IEEE, n.d.: pp. 571–576. https://doi.org/10.1109/AMC.2004.1297931.

[17] T. Brezina, L. Brezina, J. Vetiska, Improvement of heavy machine tool dynamics by passive dynamic vibration absorber, MM Sci. J. 2015 (2015) 838–842. https://doi.org/10.17973/MMSJ.2015_12_201545.

[18] S.M.R. Rasid, T. Mizuno, Y. Ishino, M. Takasaki, M. Hara, D. Yamaguchi, Design and control of active vibration isolation system with an active dy–namic vibration absorber operating as accelero–meter, J. Sound Vib. 438 (2019) 175–190. https://doi.org/10.1016/j.jsv.2018.09.037.

[19] K. Mori, D. Kono, I. Yamaji, A. Matsubara, Vibration Reduction of Machine Tool Using Viscoelastic Damper Support, Procedia CIRP. 46 (2016) 448–451. https://doi.org/10.1016/j.procir.2016.03.129.

[20] B. Niu, N. Feng, E. Lund, Y. Leng, Discrete material optimization of composite structures subjected to initial excitation for minimum residual vibration, Thin-Walled Struct. 173 (2022) 108901. https://doi.org/10.1016/j.tws.2022.108901.

[21] D. Kono, T. Inagaki, A. Matsubara, I. Yamaji, Stiffness model of machine tool supports using contact stiffness, Precis. Eng. 37 (2013) 650–657. https://doi.org/10.1016/j.precisioneng.2013.01.010.

[22] A machine foundation on clay soil of different degrees of saturation, Case Stud. Constr. Mater. 17 (2022) e01327. https://doi.org/10.1016/j.cscm.2022.e01327.

[23] O. Khalaj, R. Zakeri, S.N.M. Tafreshi, B. Mašek, C. Štadler, The Effect of a Rubber Sheet on the Dynamic Response of a Machine Foundation Located over a Small Thickness of Soil Layer, IOP Conf. Ser. Earth Environ. Sci. 906 (2021) 012044. https://doi.org/10.1088/1755-1315/906/1/012044.

[24] M.K. Marichelvam, K. Kandakodeeswaran, M. Geetha, Development of hybrid composite materials for machine tool structures, Mater. Today

Proc. 47 (2021) 6746–6751. https://doi.org/10.1016/j.matpr.2021.05.125.

[25] I.G. Akande, M.A. Fajobi, O.A. Odunlami, O.O. Oluwole, Exploitation of composite materials as vibration isolator and damper in machine tools and other mechanical systems: A review, Mater. Today Proc. 43 (2021) 1465–1470. https://doi.org/10.1016/j.matpr.2020.09.300.

[26] H.-C. Möhring, C. Brecher, E. Abele, J. Fleischer, F. Bleicher, Materials in machine tool structures, CIRP Ann. 64 (2015) 725–748. https://doi.org/10.1016/j.cirp.2015.05.005.

[27] Y. Zhu, Y. Wu, H. Bai, Z. Ding, Y. Shao, Research on Vibration Reduction Design of Foundation with Entangled Metallic Wire Material under High Temperature, Shock Vib. 2019 (2019) 1–16. https://doi.org/10.1155/2019/7297392.

[28] E. Rivin, Passive Vibration Isolation, Appl. Mech. Rev. 57 (2004) B31–B32. https://doi.org/10.1115/1.1849173.

[29] T. Kato, K. Kawashima, T. Funaki, K. Tadano, T. Kagawa, A new, high precision, quick response pressure regulator for active control of pneumatic vibration isolation tables, Precis. Eng. 34 (2010) 43–48. https://doi.org/10.1016/j.precisioneng.2009.01.008.

[30] A. Preumont, M. Horodinca, I. Romanescu, B. de Marneffe, M. Avraam, A. Deraemaeker, F. Bossens, A. Abu Hanieh, A six-axis single-stage active vibration isolator based on Stewart platform, J. Sound Vib. 300 (2007) 644–661. https://doi.org/10.1016/j.jsv.2006.07.050.

[31] C.F.J. Geerts, G.H. Veldhuizen, Precision copying machine for variable-curvature surfaces, Precis. Eng. 6 (1984) 9–11. https://doi.org/10.1016/0141-6359(84)90065-5.

[32] J. Patel, D. Panchal, H. Patel, D.H. Pandya, Harmonic analysis of single point cutting tool with multi-layer passive damping (MLPD) technique, Mater. Today Proc. 44 (2021) 625–628. https://doi.org/10.1016/j.matpr.2020.10.601.

[33] J. Lee, C.E. Okwudire, Reduction of vibrations of passively-isolated ultra-precision manufacturing machines using mode coupling, Precis. Eng. 43 (2016) 164–177. https://doi.org/10.1016/j. precision eng.2015.07.006.

[34] C.E. Okwudire, J. Lee, Minimisation of the residual vibrations of ultra-precision manufacturing machines via optimal placement of vibration isolators, Precis. Eng. 37 (2013) 425–432. https://doi.org/10.1016/j.precisioneng.2012.11.005.

[35] M. Whittle, R.J. Atkin, W.A. Bullough, Fluid dynamic limitations on the performance of an elec–trorheological clutch, J. Nonnewton. Fluid Mech. 57 (1995) 61–81. https://doi.org/ 10.1016/0377-0257(94)01296-T.

[36] P.G. Benardos, G.C. Vosniakos, Predicting surface roughness in machining: A review, Int. J. Mach. Tools Manuf. 43 (2003) 833–844. https://doi.org/10.1016/S0890-6955(03)00059-2.

[37] G. Miragliotta, The power of dimensional analysis in production systems design, Int. J. Prod. Econ. 131 (2011) 175–182. https://doi.org/10.1016/j.ijpe.2010.08.009.

[38] J.S. Rapur, R. Tiwari, Experimental Time-Domain Vibration-Based Fault Diagnosis of Centrifugal Pumps Using Support Vector Machine, ASCE-ASME J Risk Uncert Engrg Sys Part B Mech Engrg. 3 (2017). https://doi.org/10.1115/1.4035440.

[39] W.M. Winslow, Induced Fibration of Suspensions, J. Appl. Phys. 20 (1949) 1137–1140. https://doi.org/ 10.1063/1.1698285.

[40] T. Hao, A. Kawai, F. Ikazaki, The Yield Stress Equation for the Electrorheological Fluids, Langmuir. 16 (2000) 3058–3066. https://doi.org/10.1021/la990881r.

[41] A.A. Jadhav, D.A. Suryawanshi, S.B. Zope, S.S. Gawade, Design and Development of Electro-Rheological Fluid [ERF] Machine Tool Mount, in B B Aahuja (Ed.), Proc. 6th Int. 27th All India Manuf. Technol. Des. Res. Conf., COEPune, College of Engineering Pune, 2016: pp. 723–727.

[42] A.A. Jadhav, S.B. Zope, D.A. Suryawanshi, dy–namic response analysis of Electro-Rheological Fluid [ERF] dynamic response analysis of Electro-Rheological Fluid, in: I. 2018 (Ed.), ICOVP, 13th Int. Conf. Vib. Probl., ICOVP IIT Guwahati, IIT Guwahati, 2018.

[43] J. Kim, J.Y. Kim, S.B. Choi, Material charac–terization of ER fluids at high frequency, J. Sound Vib. 267 (2003) 57–65. https://doi.org/10.1016/S0022-460X(02)01411-6.

[44] L. Pahlavan, J. Rezaeepazhand, Dynamic response analysis and vibration control of a cantilever beam with a squeeze-mode electrorheological damper, Smart Mater. Struct. 16 (2007) 2183–2189. https://doi.org/10.1088/0964-1726/16/6/021.

[45] D. Predeepkumar, V. Muralidharan, S.S. Hameed, multi-point tool condition monitoring system - a comparative study, FME Transactions (2022) 50,193-201, http://doi.org/10.5937/ fme2201193K

[46] Sadredine, Nouredine and Cherif, Modeling and Experimental Validation of Dynamic Response of the Cutting Tool in Turning Operations, FME Transactions (2020) 48, 454-459. http://doi.org/10.5937/fme2002454S

NOMENCLATURE

ERF	Electrorheological fluid
ER Effect	Electrorheological effect
ERFDF	Electrorheological fluid damper foundation
CBM	Condition-based monitoring
SAD	Semi-active damper
PTFE	Polytetrafluoroethylene

Greek symbols

ζ	Damper factor
$\mathbf{Ę}$	ER Effect constant

ДИЗАЈН И РАЗВОЈ НОВЕ ПОДЕСИВЕ ЕЛЕКТРОРЕОЛОШКЕ ТЕЧНОСТИ (ЕРФ) ПРИГУШИВАЧА ЗА УБЛАЖАВАЊЕ ЗАОСТАЛИХ ВИБРАЦИЈА У МАШИНСКИМ АЛАТИМА

А.А. Цадхав, С.В. Зоп, Р.Р. Малаги, Д.А. Сурјаванши

Преостале вибрације у алатним машинама ометају прецизност и продуктивност. Слабљење заосталих вибрација је деценијама била индустријска брига. У међувремену, шема вибрација заосталих вибрација открива да способности пригушења потпорног темеља претежно утичу на њих. Због тога је уметање амортизера на било које друго место на машини (као што је машински стуб) неефикасно. Дакле, потребно је проверити обим уметања клапне у основу машине. Међутим, конвенционални системи за монтажу машина (бетонски темељ и гумени носачи) подједнако реагују на све променљиве уносе. Оба ова јата су резултирала неадекватним пригушивањем и можда лошом прецизношћу. Овај рад даје модел прве генерације полуактивно-вискозног пригушивача (ЕРФ дампер-темељ) са подесивим пригушењем које олакшава уградњу машине. Контролисано експериментисање излагањем развијене основе пригушивача ексцитацији машине за струг средњег оптерећења потврђује њену ефикасност и постиже слабљење од преко 48% у поређењу са конвенционалном бетонском подлогом.